frontiers in Earth Science

ORIGINAL RESEARCH
published: 27 August 2018
doi: 10.3389/feart.2018.00126

Contribution of Saharan Dust to Ion Deposition Loads of High Alpine Snow Packs in Austria (1987–2017)

Marion Greilinger[1,2], Gerhard Schauer[3], Kathrin Baumann-Stanzer[3,4], Paul Skomorowski[3,4], Wolfgang Schöner[5] and Anne Kasper-Giebl[2]*

[1] Climate Monitoring and Cryosphere, Central Institution for Meteorology and Geodynamics, Vienna, Austria, [2] Environmental and Process Analytics, Institute of Chemical Technologies and Analytics, Vienna University of Technology, Vienna, Austria, [3] Sonnblick Observatory, Central Institution for Meteorology and Geodynamics, Salzburg, Austria, [4] Environmental Meteorology, Central Institution for Meteorology and Geodynamics, Vienna, Austria, [5] Institute of Geography and Regional Research, University of Graz, Graz, Austria

We investigate the influence of Saharan dust on the chemical composition and deposition loads of a 31-year long snow chemistry data set (1987–2017) of high alpine snow packs situated close to the Sonnblick Observatory, a global GAW (Global Atmospheric Watch) station, in the National Park Hohe Tauern in the Austrian Alps. Based on the snow pack of the winter accumulation period 2015/2016, when two Saharan dust events were visible by a reddish color of the snow, we define a pH $>$ 5.6 together with a Ca^{2+} concentration $>$ 10 μeq/l as thresholds to identify Saharan dust affected snow layers. This criterion is checked with an intercomparison with trajectories and on-line aerosol data determined at the Sonnblick Observatory. This check was extended to the accumulation periods 2014/2015 and 2016/2017 before the whole time series is investigated regarding the contribution of Saharan dust to ion deposition loads. Especially Mg^{2+}, Ca^{2+}, and H^{+} depositions are strongly affected by Saharan dust input causing, as average values across the 30 years period, increased Mg^{2+} (25%) and Ca^{2+} (35%) contributions of affected snow layers, while the contribution to the snow water equivalent was only 11%. For H^{+} Saharan dust affected snow layers show a much lower contribution (2%) while the contribution of other ions is well comparable to the deposition amount expected according to the snow water equivalent of affected snow layers. The pH range of Saharan dust affected snow layers covers 5.58–7.17, while the median value of all samples is 5.40. The long term trends of ion deposition are not affected by the deposition of Saharan dust.

Keywords: mineral dust, Saharan dust, snow chemistry, high alpine snow pack, deposition loads

OPEN ACCESS

Edited by:
Pavla Dagsson-Waldhauserova, Agricultural University of Iceland, Iceland

Reviewed by:
Silvia Becagli, Università degli Studi di Firenze, Italy
Dragana S. Đorđević, University of Belgrade, Serbia

****Correspondence:***
Marion Greilinger
marion.greilinger@zamg.ac.at

Specialty section:
This article was submitted to Cryospheric Sciences, a section of the journal Frontiers in Earth Science

Received: *07 March 2018*
Accepted: *10 August 2018*
Published: *27 August 2018*

Citation:
Greilinger M, Schauer G, Baumann-Stanzer K, Skomorowski P, Schöner W and Kasper-Giebl A (2018) Contribution of Saharan Dust to Ion Deposition Loads of High Alpine Snow Packs in Austria (1987–2017). Front. Earth Sci. 6:126. doi: 10.3389/feart.2018.00126

INTRODUCTION

Deserts serve as a major source for aerosols in the atmosphere with mineral dust as a main contributor to primary aerosol mass. Especially the Sahara, the largest desert in the world, contributes roughly half of the primarily emitted aerosol mass found in the atmosphere and is thus the world's largest source for Aeolian soil dust (Prospero, 1996; Goudie and Middleton, 2001 and references therein). Once in the atmosphere, desert dust can be transported over thousands of kilometers via synoptic wind patterns to regions far beyond (e.g., Prospero, 1996; Moulin et al., 1997). Online aerosol measurements conducted since 2013 at Austria's high alpine Sonnblick

Observatory, listed as a global station within the Global Atmospheric Watch Program of the World Meteorological Organization, suggest up to 30 days per year with the influence of mineral dust. Due to the predominant contribution of dust origination from the Sahara the term Saharan dust will be used within this paper. Transported dust can be removed from the atmosphere through wet and dry deposition processes.

If dust is deposited on mountain snow packs it causes several direct and indirect effects. Firstly, Saharan dust deposited onto snow surfaces decreases the albedo due to a darkening of the surface and consequently higher absorption of solar radiation, leading to an earlier removal of the snow cover or increased glacier melt-off (Goudie and Middleton, 2001; Field et al., 2010). This triggering of faster and earlier melt-off due to the dust deposition can potentially result in a lower total and less late-season water supply (Field et al., 2010) due to melt-off already during the season. This is especially important in areas where water supply is scarce. A more recent study of Gabbi et al. (2015) investigated the long-term effect of snow impurities, mainly Saharan dust and Black Carbon, on albedo and glacier mass balance and found that their presence lowered the albedo by 0.04–0.06, thereby increasing melt by 15–19% and reducing the mean annual mass balance.

Secondly, dust plays an important role in the control of global and regional biogeochemical cycles. These effects have been studied mostly in seawater or the Amazonas basin. For seawater especially P and Fe are supposed to be the main actors to estimate the contribution of atmospheric inputs stimulating the productivity of oceanic plankton, thus accelerating CO_2 uptake and stimulating N_2-fixation (Gruber and Sarmiento, 1997; Field et al., 2010; Schulz et al., 2012). For the Amazonas basin, Swap et al. (1992) and Rizzolo et al. (2017) showed that especially Fe^{3+}, Na^+, Ca^{2+}, K^+, and Mg^{2+} are the main constituents introduced via Saharan dust, acting as fertilizer or micronutrients essential for plant growth by offsetting the losses of nutrients due to leaching or weathering of the soil. Many other studies propose the significant influence of Saharan dust on microbiology, nutrient supply, acid neutralization and geochemistry in Europe as well. Avila et al. (1998) for example found that red rains, indicating Saharan dust influence, are important for biogeochemical consequences of a Holm oak forest in Catalonia, Spain, due to addition of nutrient elements such as K^+, Ca^{2+}, and Mg^{2+} and input adding to the neutralizing capacity of the soils in the catchment. The effect of Saharan dust on high alpine snow biogeochemistry is still poorly investigated although many studies propose that the ionic composition and deposition load of snow is of high biogeochemical interest because snow serves as interface where the water and nutrient cycle interact (De Angelis and Gaudichet, 1991; Kuhn, 2001). Marchetto et al. (1995) just showed that for alpine lakes in areas of low weathering rocks, such as silicate rocks also present at the site investigated in this study, lake chemistry, including acidity and alkalinity, is mainly determined by atmospheric deposition. Additionally it is well known that Saharan dust alters the chemical composition and neutralizing capacity of precipitation and, if deposited, also of snow packs and thus influences surface water chemistry (De Angelis and Gaudichet, 1991; Rogora et al., 2004). If the chemical composition of high alpine snow packs is investigated the main ions analyzed generally are Cl^-, SO_4^{2-}, NO_3^-, NH_4^+, Na^+, K^+, Mg^{2+}, Ca^{2+} as well as the pH and conductivity. Their origin can be assigned to different sources like anthropogenic sources, sea salt or mineral dust (Maupetit and Delmas, 1994). Greilinger et al. (2016) who analyzed the long-term series of snow chemistry data used in this study found three different clusters of ions representing different types of origin. Thereby one cluster representing mineral dust sources was found, positively correlated with Ca^{2+} and Mg^{2+} together with a negative correlation for H^+, representing the alkaline characteristics of mineral dust. Findings are comparable to results from Maupetit and Delmas (1994). It can be proposed that increased Ca^{2+} and Mg^{2+} concentrations change the chemical characteristics of the samples, especially the pH value.

Thirdly, Aeolian dust and as such also Saharan dust, is used by microorganisms to disperse and colonize new habitats. It is assumed, that microorganisms that are able to survive in the harsh conditions of the Sahara and the atmosphere during transport may also be able to colonize other sites with comparably challenging conditions such as the high Alps (Chuvochina et al., 2011) or the Himalaya (Zhang et al., 2008). It has been shown in a recent study of Weil et al. (2017) that those microbial dust passengers introduced to high alpine snow packs via Saharan dust can favor a rapid microbial contamination of sensitive habitats after snowmelt.

Due to the described effects of Saharan dust on mountain snow packs, the main purpose of this paper is to investigate the intensity and frequency of Saharan dust deposited in high alpine snow packs via a retrospective evaluation of a unique high alpine snow chemistry data set of 31 years (1987–2017) and to quantify the impact of these events on the deposition load.

According to Psenner (1999), who investigated the relevance of airborne dust like Saharan dust for the ecology of alpine lakes, an interdisciplinary research is necessary to elucidate the impact of dust on ecological issues. An estimation of the contribution of Saharan dust to the chemical variability of the ecosystems is not easy due to lack of quantitative studies in remote areas but cannot be neglected when dealing with acidification and recovery processes. Thus, our study provides relevant input for further investigations and conclusions, and indicates that the stochastic occurrence of Saharan dust deposition is on the long run a constant factor influencing the terrestrial and aquatic ecosystem of the Alpine region.

MEASUREMENTS AND METHODS

The study area, sampling, and measurement techniques as well as data quality issues are thoroughly described in Greilinger et al. (2016) and are only summarized shortly in this section.

Study Area

Snow profiles were sampled at the Goldbergkees (GOK), a remote glacier field, part of the Goldberggruppe at an elevation of more than 3,000 m.a.s.l. (**Figure 1**) close to the Sonnblick Observatory, listed as a global station within the Global

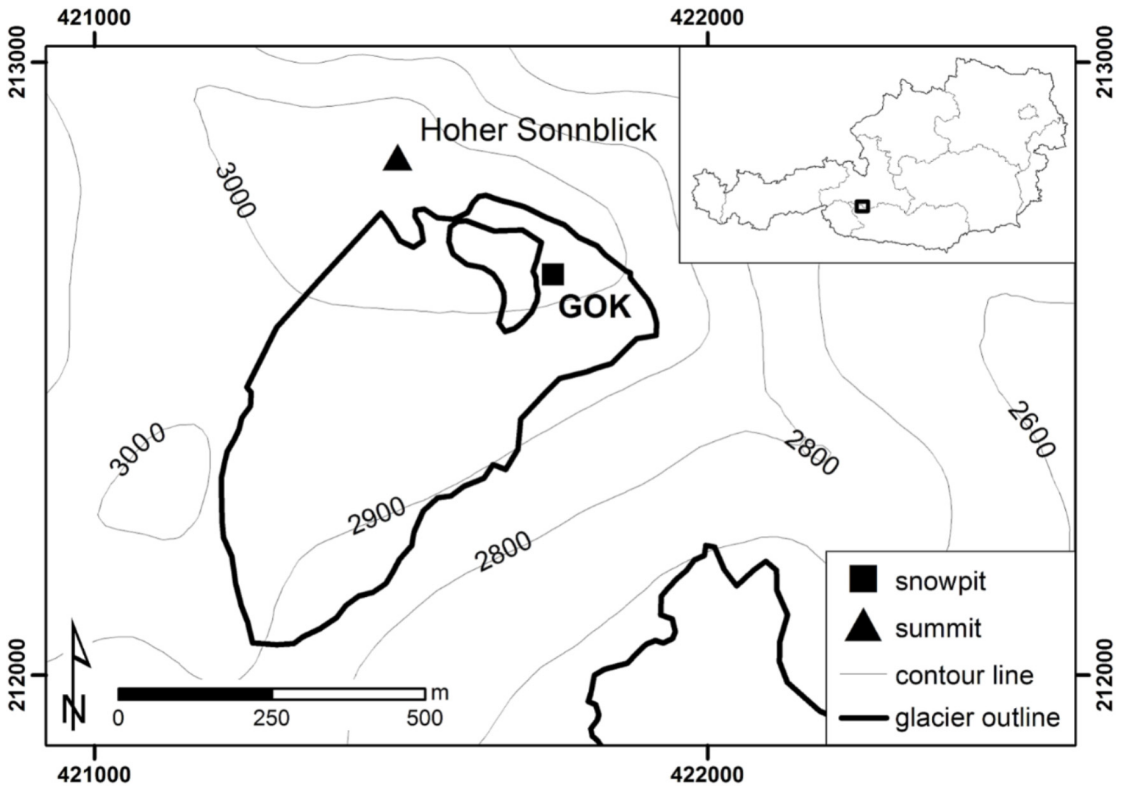

FIGURE 1 | Location of the Goldberggruppe in Austria, the sampling site Goldbergkees (GOK) on a glacier field in the Eastern Alps and of the mountain summit Hoher Sonnblick where the meteorological observatory is situated.

Atmospheric Watch Program of the World Meteorological Organization. The site is not exposed to any local anthropogenic influence.

Snow Sampling and Chemical Analysis

Snow samples representing the whole winter accumulation period are taken annually in a vertical resolution of 10 cm increments just prior to the start of significant snowmelt (usually at the end of April or the beginning of May). Just in 1997 the size of the increments was 40 cm. Note that the respective increments could either represent a portion of a single precipitation event or include mixed information of several events, depending on precipitation amount and settling of the snow cover. After digging a snow pit until the horizon when winter accumulation had started snow samples were taken with a stainless steel cylinder and stored in polyethylene bags. To avoid contamination of the samples gloves and a mask were used during sampling. Samples were taken to the lab frozen and were analyzed immediately after thawing. Analytical protocols changed slightly during the period of observation, but quality assurance was maintained by regular participation in the laboratory intercomparison of the World Data Center for Precipitation Chemistry (Global Atmosphere Watch). Conductivity and pH were determined electrochemically using a conductivity cell and a glass electrode, respectively. Anion (chloride, nitrate and sulfate) and monovalent cation (sodium, potassium, ammonium) concentrations were determined by suppressed ion chromatography. Bivalent cation (calcium, magnesium) concentrations were determined by atomic absorption spectroscopy until 1993, and only later by ion chromatography. Limits of detections (LODs) changed slightly during the years but were in the range of 0.01 and 0.015 mg/L for all ions and years, aside from sulfate and the time period until 1993, when a LOD of 0.029 mg/L was obtained. More details are given in Winiwarter et al. (1998) and Greilinger et al. (2016) including data quality control, outlier discussion and general presentation of the data.

Trajectory Analysis

In meteorology trajectories are defined as the paths of infinitesimally small particles of air. Such an air parcel, 'marked' at a certain point in space at a given time, can be traced forward or backward in time along its trajectory. In this study, air mass trajectories are calculated using the Flextra model (Stohl et al., 2001) based on meteorological data provided by ECMWF (European Centre for Medium Range Weather Forecast) with a horizontal resolution of 0.2°. The trajectories are starting from Sonnblick Observatory eight times per day (00UTC, 03UTC, 06UTC, 09UTC, 12UTC, 15UTC, 18UTC, and 21UTC) and trace the path of the air parcel backward in time for the previous 96 h, giving an indication where the major part of the air mass came from.

Aerosol Measurements

Aerosol sampling is performed via a heated (+20°C) whole air inlet designed according to GAW guidelines, with an upper size cut of 20 μm at a wind speed of 20 m/s. Details about the setup are given in Schauer et al. (2016). Episodes with a dominant influence of dust are continuously identified via the optical properties of the aerosol and the corresponding calculation of the wavelength dependence of the Single Scattering Albedo (SSA) according to Coen et al. (2003). Therefore a three-wavelength polar Nephelometer (Aurora 4000, Ecotech) was used for the determination of the light scattering coefficients at 450, 525, and 635 nm. Absorption coefficients were determined with an Aethalometer (AE33, Magee Scientific) at seven wavelengths, i.e., 370, 470, 525, 590, 660, 880, and 940 nm. A detailed description of the respective calculations can be found in Schauer et al. (2016). Based on this identification and on particulate matter (PM) concentrations a "dust index" is calculated on a routine base. A positive DI is reported when an influence of dust is identified for at least eight half hourly means during the day with a PM concentration above 5 $\mu g/m^3$. Mass concentrations of particulate matter are determined via a combination of nephelometry and β-attenuation (Sharp 5030, Thermo Scientific).

RESULTS

Several studies (e.g., Maupetit and Delmas, 1994; Greilinger et al., 2016) investigated the qualitative source assignments of high alpine snow packs using principal component analysis (PCA) and identified a factor related to Ca^{2+}, Mg^{2+} and the pH, being indicative for a marked contribution of Saharan dust. However, to get quantitative information on the contribution of Saharan dust to the respective ion composition or annual deposition loads the investigation of single snow layers is essential.

Identification of Saharan Dust Affected Snow in the Snowpack of the Winter Accumulation Period 2015/2016

Chemistry of the Snow Pack GOK2016

In the snowpack representing the winter accumulation period from September 2015 to April 2016 (=GOK2016), reddish colored snow layers where observed during sampling in about 120–160 cm depth (compare picture of the snow pack in **Figure 2**). Still, this depth has to be regarded as an approximate value and can be inaccurate by about 10–15 cm. This is because sampling is performed in an up to 2 m wide snow pit and the actual sampling of the 10 cm increments might be 0.5–1 m off the position where the depth, the snow morphology and also the color were determined. This "red snow," along the lines of "red rain" as used by Avila et al. (1998), is interpreted as an indicator of long-range transport of mineral dust, most likely originating from the Sahara. Although the color can vary from yellowish to brownish and up to now reddish, we stick to the term "red snow" throughout the paper.

To identify potential Saharan dust affected snow by chemical analysis, we build on a 2-step approach based on Rogora et al. (2004). They investigated a 15- to 20-year long time series of rain water chemistry data of Northwest Italy and grouped rain events in acid and alkaline events with a pH of 5.6 as the threshold, representing the pH of pure water equilibrated with atmospheric CO_2. Although a pH of 5.6 still represents acid conditions, the samples denoted as "alkaline" feature comparable high pH. Within this work we will use the same notation as Rogora et al. (2004) and denote "alkaline increments" to 10 cm sample increments featuring pH > 5.6. After the identification of the alkaline events, Rogora et al. (2004) characterized Saharan dust episodes, as a subgroup of the alkaline events, via a high Ca^{2+} and alkalinity content, but no strict values are given for this classification.

Using the pH > 5.6 threshold we identified five alkaline increments of 10 cm (**Table 1**). This is one more (350–360 cm) than visually identified as "red snow." These alkaline increments can be further distinguished via their chemical composition. Either an elevated Ca^{2+} concentration often accompanied by increased concentration of the other ions, representing a Saharan dust influence, or an increased NH_4^+ concentration most likely associated to anthropogenic sources in agriculture (Greilinger et al., 2016) was noted. Both, Ca^{2+} and NH_4^+ act as important neutralizing agents for the anions SO_4^{2-} and NO_3^- (Das et al., 2005). The chemical composition of all 10 cm increments is given in **Table 1** and **Figure 2** (right).

Ca^{2+} and Mg^{2+} concentrations of the increments 130–140 cm, 140–150 cm, and 350–360 cm were all above the 87th percentile. The 160–170 cm increment showed elevated concentrations as well, but concentrations of NH_4^+ and NO_3^- were much more pronounced than Ca^{2+} and are the highest observed for the whole snow pack. The pH was actually just slightly above the threshold of 5.6. The 150–160 cm increment showed markedly elevated concentrations of NH_4^+, NO_3^- and SO_4^{2-}, and just slightly elevated Ca^{2+} concentrations. Based on these results we can separate the alkaline increments in one fraction dominated by increased Ca^{2+} concentrations (increments from 130 to 140 cm, 140 to 150 cm, and 350 to 360 cm) and one fraction dominated by increased NH_4^+ concentrations (150–160 cm). As the 160–170 cm increment is featuring both characteristics highest concentrations for NH_4^+ and NO_3^-, but also elevated concentrations of Ca^{2+}, it cannot be clearly assigned to one of the two categories.

Taking 10 μeq/l as threshold (higher than the 85th percentile, close to the arithmetic mean of 8.9 μeq/l and below the concentrations of the six samples showing the upper and detached range of the frequency distribution) four 10 cm increments (130–140 cm, 140–150 cm, 160–170 cm, and 350–360 cm) can be classified as affected by Saharan dust in the 2015/2016 snow pack. This fits nicely to the classification of the alkaline increments given above as it does not include the one from 150 to 160 cm, dominated by increased NH_4^+ concentration. Furthermore the increment at the bottom of the snow pack (350–360 cm) is identified, although it was not visible as 'red snow.' For completeness we want to point out that two increments show Ca^{2+} concentrations higher than 10 μeq/l but a pH less than 5.6. Thus the combination of the pH criterion and the Ca^{2+} threshold is mandatory.

TABLE 1 | Ion concentrations, pH, conductivity, and ion sum of every single 10 cm increments of the snow pack from the accumulation period September 2015 to April 2016.

Snow depth (cm)	Ion concentration (μeq/l)									Σ ions (μeq/l)	pH	Conductivity (μS/cm)
	Na^+	NH_4^+	K^+	Mg^{2+}	Ca^{2+}	Cl^-	NO_3^-	SO_4^{2-}	H^+			
0–10	5.96	16.38	2.25	1.46	5.63	5.20	14.09	6.02	2.67	59.66	5.39	9.19
10–20	1.43	39.19	0.72	0.81	5.20	1.53	21.44	14.24	3.77	88.33	5.24	13.36
20–30	1.28	42.99	0.87	0.74	4.21	1.70	22.49	21.31	4.32	99.91	5.17	17.63
30–40	1.56	3.29	0.59	0.16	0.64	1.46	2.00	2.74	5.08	17.52	5.10	4.02
40–50	0.62	0.83	0.22	0.05	0.27	0.45	0.28	0.74	2.43	5.89	5.21	1.91
50–60	0.63	0.76	0.22	0.10	0.53	0.57	0.69	0.68	2.43	6.61	5.21	2.23
60–70	0.85	0.38	0.31	0.07	0.38	1.01	0.63	1.35	4.16	9.14	5.18	1.94
70–80	0.99	1.99	0.34	0.62	1.98	1.01	2.26	1.51	3.23	13.93	5.29	2.13
80–90	0.88	7.39	0.21	0.40	0.73	1.15	5.86	2.08	4.68	23.38	5.24	3.36
90–100	0.50	12.89	0.15	0.27	0.73	0.60	9.07	2.95	4.79	31.95	5.23	4.56
100–110	0.58	11.55	0.22	0.26	0.55	0.95	6.09	1.75	4.03	25.98	5.29	3.66
110–120	0.41	12.60	0.34	0.65	1.26	0.44	7.02	1.82	2.92	27.46	5.43	3.55
120–130	3.54	14.53	1.24	2.21	6.29	3.56	6.47	2.87	3.69	44.40	5.43	4.91
130–140	**16.89**	**22.94**	**2.92**	**13.40**	**171.51**	**19.64**	**28.23**	**33.70**	**0.07**	**309.30**	**7.17**	**28.80**
140–150	**2.77**	**17.11**	**0.56**	**3.44**	**40.87**	**3.32**	**14.01**	**6.43**	**0.32**	**88.83**	**6.49**	**8.38**
150–160	**1.82**	**29.59**	**0.38**	**1.15**	**5.17**	**1.91**	**19.40**	**5.00**	**1.86**	**66.28**	**5.73**	**6.27**
160–170	**5.20**	**47.98**	**1.10**	**3.90**	**24.42**	**3.72**	**41.33**	**16.67**	**2.05**	**146.37**	**5.74**	**13.02**
170–180	0.74	10.50	0.37	0.28	1.35	0.89	8.09	4.09	6.34	32.65	5.25	3.07
180–190	2.83	4.25	0.77	1.43	11.72	2.30	8.06	7.40	5.44	44.20	5.33	3.87
190–200	0.66	4.96	0.08	0.29	0.52	0.92	3.28	0.60	4.96	16.27	5.37	1.04
200–210	2.06	8.16	0.47	0.97	4.18	1.88	5.91	3.27	4.28	31.18	5.40	2.64
210–220	2.29	4.71	0.38	0.97	11.75	2.03	5.81	3.00	7.61	38.55	5.15	3.84
220–230	0.36	2.92	0.18	0.14	0.96	0.27	5.95	2.27	10.92	23.97	5.04	3.80
230–240	0.47	2.46	0.18	0.49	2.93	0.61	7.53	2.05	9.30	26.02	5.11	3.31
240–250	0.37	3.75	0.16	0.44	3.17	1.03	6.57	1.21	6.05	22.75	5.25	2.31
250–260	0.37	7.21	0.22	0.12	1.02	0.49	9.64	1.75	7.79	28.61	5.14	3.70
260–270	0.32	1.08	0.08	0.30	2.38	0.45	2.77	0.46	12.20	20.04	5.00	3.73
270–280	4.41	1.89	1.34	1.31	6.15	4.61	5.57	1.42	8.84	35.54	5.14	3.64
280–290	3.42	3.41	0.67	1.29	3.53	3.55	8.27	2.51	12.81	39.46	5.01	5.10
290–300	1.03	1.16	0.37	0.32	1.96	1.81	3.66	1.17	6.72	18.20	5.29	1.45
300–310	1.12	1.73	0.42	0.56	2.51	1.73	4.71	1.70	12.69	27.17	5.03	3.74
310–320	0.65	1.36	0.24	0.67	4.41	0.96	4.78	1.76	5.41	20.24	5.40	1.32
320–330	0.49	1.59	0.07	0.67	2.45	0.63	5.79	1.04	6.45	19.18	5.20	2.45
330–340	0.80	3.74	0.16	0.59	2.30	0.98	7.01	1.41	6.45	23.44	5.20	2.70
340–350	0.30	4.47	0.08	1.52	7.20	0.42	5.06	1.25	4.19	24.49	5.44	1.28
350–360	**0.35**	**2.75**	**0.08**	**1.90**	**11.57**	**0.49**	**3.89**	**2.09**	**0.70**	**23.82**	**6.22**	**1.12**
360–370	0.51	2.08	0.19	0.12	1.07	0.73	2.39	1.41	7.97	16.47	5.13	2.37
370–380	0.28	1.01	0.07	0.12	0.48	0.33	3.38	0.20	5.39	11.26	5.30	0.99
380–390	0.46	2.98	0.34	0.32	0.92	0.70	1.92	1.17	8.08	16.89	5.21	1.71
390–400	0.46	4.65	0.09	0.15	0.79	0.67	2.35	1.12	7.21	17.49	5.26	1.55
Min	0.28	0.38	0.07	0.05	0.27	0.27	0.28	0.20	0.07	5.89	5.00	0.99
1st quantile	0.47	1.97	0.18	0.27	0.89	0.61	3.36	1.24	3.58	18.03	5.17	2.08
2nd quantile	0.77	4.00	0.33	0.58	2.42	1.00	5.89	1.79	5.02	25.24	5.25	3.46
Mean	1.77	9.13	0.49	1.12	8.89	1.92	8.09	4.16	5.51	41.07	5.36	4.74
3rd quantile	1.88	11.81	0.57	1.19	5.31	1.89	8.14	3.07	7.31	38.78	5.39	4.16
Max	16.89	47.98	2.29	13.40	171.51	19.64	41.33	33.70	12.81	309.30	7.17	28.80

Bold values represent the alkaline increments using a pH > 5.6 for identification.

Comparison With Backward Trajectories and Aerosol Measurements

Based on the recording of precipitation events and snow height measurements the increments affected by Saharan dust can roughly be assigned to respective time periods. To confirm the influence of Saharan dust during these time periods backward trajectories and on-line aerosol measurements are used.

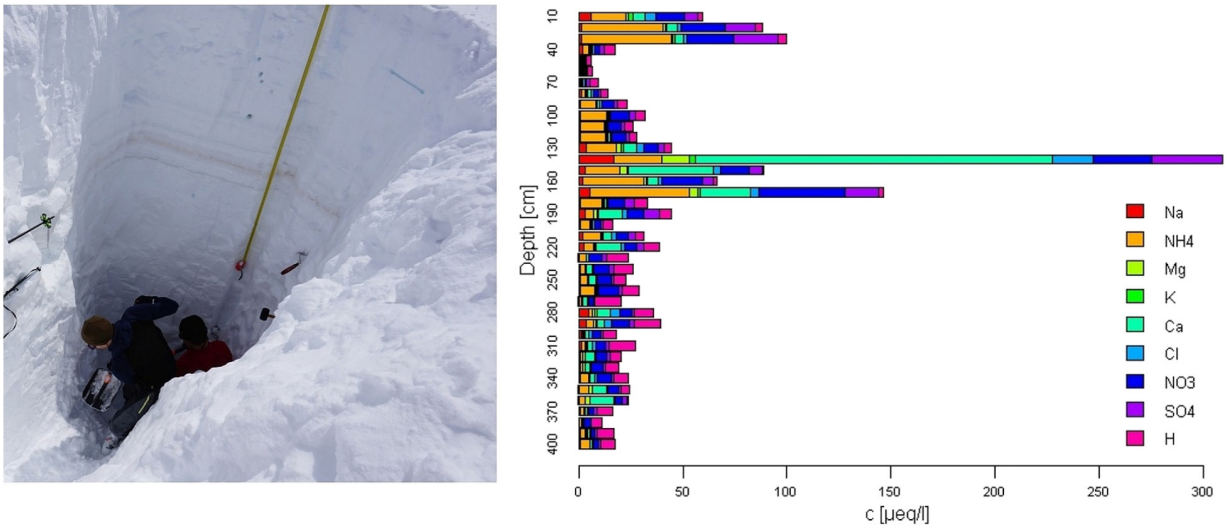

FIGURE 2 | (Left) Picture of the snow pack where the reddish Saharan dust snow layer in a depth of 120–140 cm is clearly visible. **(Right)** Chemical composition of every 10 cm increment of the whole snow pack showing Saharan dust layers from 120 to 180 cm with increased ion concentrations of especially Ca^{2+}.

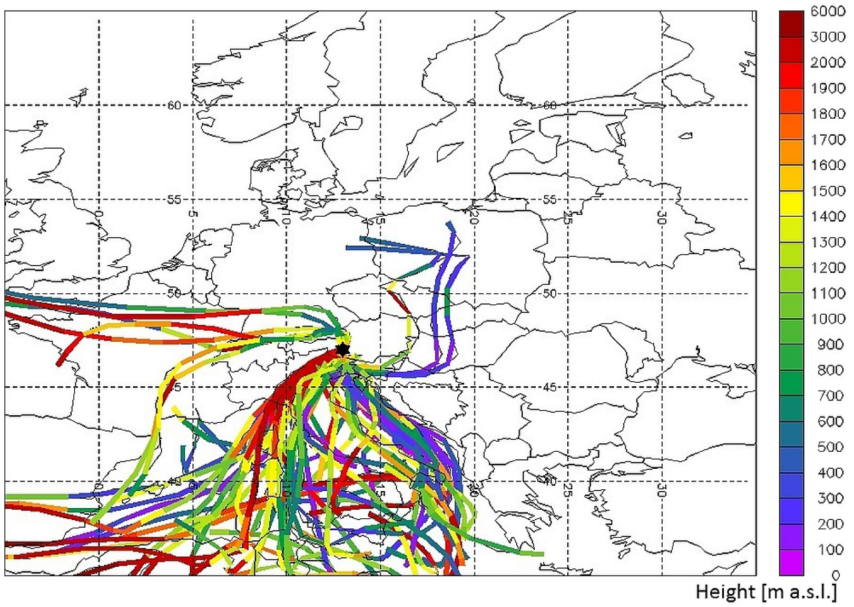

FIGURE 3 | Ninety-six hours backward trajectories starting from the Sonnblick Observatory every 3 h between 31 March 2016 00UTC and 8 April 2016 21UTC. Trajectories from the South reveal that Saharan dust occurrence at the sampling site during that time is very likely.

The 10 cm increments from 130 to 150 cm and 160 to 170 cm represent precipitation events occurring in spring and can be assigned to a strong Saharan dust event in April, which is documented by backward trajectories for the period from 31 March 2016 00UTC until 8 April 2016 21UTC given in **Figure 3**. The frame of the image includes only the coastal area of Egypt and Tunisia and not the Sahara as such because the high resolution meteorological data of the ECMWF (horizontal resolution of 0.2°) is not available further south. Backward trajectories running southward out of the frame and descending from high altitudes are highly likely to come from the Sahara. On-line aerosol measurements at Sonnblick Observatory indicate that this event can be separated in two episodes. The first episode lasts from 31 March until 3 April 2016 and the second one, which was three times stronger regarding the mass concentration of particulate matter starting at 4 April 2016. Due to wind drift accumulation and precipitation, causing a slight increase in snow height in-between the episodes (measured by an automatic ultrasonic sensor next to the sampling site and shown in **Supplementary Figure 1**) it is plausible that they are separated in the snow

TABLE 2 | Years and depth where visible red snow was recorded in handwritten protocols and photographs during sampling and associated snow sample increments featuring a pH > 5.6 and a Ca^{2+} concentration of >10 μeq/l.

	Year	Depth recorded in protocols (cm)	Depth of snow sample increments (cm)	Ca^{2+} > 10 μeq/l
1	1987	80–84	75–85	+
2	1987	130	115–125	+
3	1987	370	365–375	+
4	1991	106–109	100–110	+
5	1992		210–220	+
6	1993	Snow surface	–	
7	1994	27–32	20–30 and 30–40	+
8	1995	290–292	280–290	+
9	1995	351–351.5*	–	–
10	1996	9–10	10–20	+
11	1996	130–140	130–140	+
12	1996	220–230	210–220	+
13	1997	368–370**	–	–
14	1997	377–381**	–	–
15	1997	520–527	500–540	+
16	2000	234–240	230–240	+
17	2003	240–241	240–250	+
18	2007	200	210–220	+
19	2012	150	150–160	+
20	2014	95–100	90–100	+
21	2014	184–189	180–190	+
22	2016	120–130	130–140	+
23	2016	130–140	140–150	+

**Indicates that there is a note in the metadata that Saharan dust was not continuously present. **Indicates that in 1997 the height of the sampling increments was 40 cm, leading to a loss of information due to dilution. The pH of these layers was 5.48, hence they slightly missed the pH-criterion.*

cover by one 10 cm increment. The 350–360 cm increment, showing an increased pH and a slight increase in the ion sum and Ca^{2+} concentration, represent snow samples from autumn (November and possibly also December 2015), which were concentrated in this depth due to an almost stable snow cover height during this time. Backward trajectories as well as on-line aerosol measurements indicate an influence of Saharan dust, though much lower than in spring 2016, during several days in November and December 2015 (**Supplementary Figures 2–4**) and thus justify the chemical identification of this increment.

Concluding, reasonable agreement of the identification of Saharan dust episodes between backward trajectories, aerosol measurements and the snow pack was obtained. This allows to extend the presented approach to the entire data set to retrospectively identify Saharan dust affected samples of snow packs back until 1987.

Retrospective Identification of Saharan Dust Layers

For 12 years (1987, 1991–1997, 2000, 2003, 2014, and 2016) hand written records reveal the presence of visible red snow in the respective snow pack. Besides, photographs of the snow packs are available since 2004, except for 2015. They show red snow for the years 2007, 2012, 2014, and 2016. Thus in total 23 layers within 14 years feature visually present red snow (listed in **Table 2**). Their position within the snow pack is reported in the column named "depth recorded in protocols." The respective depth of affected increments identified via the pH and Ca^{2+} criterion is also reported in **Table 2** in the column "depth of snow sample increments." Thereby it is important to mention that the recorded snow depth need not correspond exactly to the sample increments of the same layer due to variations in the snow pit as described earlier. Additionally it is possible, that the Saharan dust layer (SDL) is split into two 10 cm sample increments or that it is much thinner than the sample increment, both leads to a dilution of the concentration in the affected layer.

Table 2 shows that 19 out of the 23 layers with red dust identified by visual inspection are identified using the pH > 5.6 and Ca^{2+} > 10 μeq/l thresholds. Reasons for this mismatch can be easily given. In 1995 it was recorded that the colored layer was not continuously present across the width of the snow pit. Hence it is not contradicting that Ca^{2+} concentrations were not markedly elevated. In 1997 sample increments were 40 cm instead of 10 cm, leading to a dilution and thus to a poorer sensitivity of the analytical approach. The respective increment showed a pH value of 5.48 which is only slightly lower than the used threshold of 5.6. In 1993 Saharan dust was visible on the snow surface but the respective increment only matched the Ca^{2+} criterion but, with a pH of 4.78, not the pH criterion. Maybe other influences on the surface (e.g., snow surface–air interactions) do play a role for the pH. Excluding those layers from the evaluation all recorded red dust layers could be verified by the chemical analysis.

The total data set covers 28 years of snow pack data (1987–2017, except 1988, 1989, and 1990 due to missing values for bivalent cations) and comprises 1,163 chemically analyzed 10 cm increments. Increments which were identified to feature Saharan dust input are here named as "SDLs," although they do not necessarily represent different stratigraphic layers or single events. Based on the chemical information we find 394 alkaline layers (equal to 34% of the whole data set) using the pH criterion only. For comparison, the mean pH of all samples is 5.44 with 75th percentile and 90th percentile values of 5.70 and 6.15, respectively. Including the Ca^{2+} criterion this number of layers decreases to 104 (equal to 9% of the whole data set or 26% of the alkaline layers) with pH values ranging from 5.58 to 7.17. As it was the case for the GOK2016 snow pack there are more sample increments chemically identified as SDLs than samples showing a visible appearance of red snow. More precisely we find five times more based on chemistry compared to the visual identification.

Some validation can be given for the accumulation periods 2014/2015 and 2016/2017, as back trajectories and on-line aerosol data are available for these years as well. In both years, no red snow was visible, but in case of the 2016/2017 period (GOK2017) one SDL was chemically identified in the lower part of the snow pack. Backward trajectories indicate the influence of Saharan dust in October 2016 and also two much weaker episodes in spring 2017 (compare **Supplementary Figures 5** and **6**). Complementary on-line aerosol measurements yielded a positive dust index during the respective time periods. Thus the SDL identified in the bottom part of the snow pack much likely represents the event in October 2016. The spring events in February and March 2017 are, using the present methods, not identified in the snow pack. Still sample increments which can be assigned to the relevant time period meet the pH criterion and show a Ca^{2+} concentration of 9.72 μeq/l, i.e., only slightly below the threshold of 10 μeq/l. Within the snow pack of the 2014/2015 accumulation period (GOK2015) no SDLs were chemically identified. Again backward trajectories and on-line aerosol data shows some influence during early winter at the end of November and beginning of December 2014 (**Supplementary Figure 7**), which is not reflected in the lowest part of the snow pack. This seems surprising, but snow height measurements revealed the absence of wet deposition during these events. During spring time the situation was similar to the conditions described for the GOK2017 and the GOK2016 snow pack. A Saharan dust influence occurred in March 2015 (backward trajectories given in **Supplementary Figure 8**) and the respective sample increments again meet the pH criterion, but were slightly below the 10 μeq/l Ca^{2+} threshold (Ca^{2+} concentration of 9.48 μeq/l). This intercomparison suggests that it is most likely that no overestimation of SDLs occurs when the criteria defined within this paper are used. Weak events might even be missed. Furthermore the influence of Saharan dust, and not just a general influence of mineral dust, is likely for all identified events.

In literature markedly higher Ca^{2+} values can be found to identify Saharan dust affected samples. Maupetit and Delmas (1994) report a value of 23.8 μeq/l for alkaline snow samples collected in the French Alps. A Ca^{2+} threshold of 20 μeq/l was also used by Schwikowski et al. (1999) to classify ice core data from an Alpine ice core (Colle Gnifetti). Of course these concentrations are strongly driven by the respective accumulation rates and thus can vary from site to site. Still we want to elucidate how sensitive the classification is to respective thresholds. If we would use a threshold of 20 μeq/l, the recovery in the chemical analysis of the visually identified reddish SDLs would decrease. Consequently the number of identified SDLs of the whole data set including all increments (not only the visually noticeable ones) decreases as shown in **Table 3**. Despite this decreasing trend the snow pack still experiences an impact of Saharan dust during more than half of the years when the 20 μeq/l criterion is used. Regarding only years with more than one identified layer (reflecting a repeated or longer lasting Saharan dust influence) more than two-thirds of the years are affected when the 10 μeq/l Ca^{2+} threshold is used. This number decreases to about one-third for the higher threshold. Obviously the level of the threshold influences the number of detected SDLs as well as years affected, but, as will be shown later, the respective deposition loads are affected much less.

TABLE 3 | Overview and seasonality of the number of Saharan dust layers (SDLs) using different Ca^{2+} thresholds of 28 years of snow pack data (1987–2017, missing data in 1988, 1989, and 1990).

	Ca^{2+} > 10 μeq/l	Ca^{2+} > 20 μeq/l
Total years investigated	28	28
Total amount of analyzed increments	1,163	1,163
Total amount of alkaline layers (pH > 5.6)	394	394
Years with minimum one SDL	26	16
Years without SDLs	2	12
Years with more than one SDL	19	8
SDLs via pH > 5.5 and Ca^{2+} threshold	104	45
SDLs in fall (September to November)	32	17
SDLs in winter (December to February)	48	19
SDLs in spring (March to April)	24	9

If the snowpack is subdivided into the different seasons of fall (September to November), winter (December to February) and spring (March and April) according to Greilinger et al. (2016), it seems as if the most Saharan dust events occur during winter (**Table 3**). This result seems surprising, since a clear fall and spring maximum can be found for Saharan dust in the atmosphere (Coen et al., 2003). Possible explanations are that potential events occurring in September might have been melted away or that they occurred without snowfall, remained airborne and were thus not deposited in or on the snow pack. Besides, during September rain is still very likely at the sampling site which might wash away already deposited Saharan dust on the snow or glacier surface or enables a deposition with rain due to rain water run-off. Events occurring in May, still accounting to the spring maximum given in Coen et al. (2003), were not captured in the snow pack analysis due to sampling end of April, latest beginning of May. Also the snow water equivalent is on average much higher for the winter period (mean over the period 1987–2017 of 663 mm) compared to fall or spring (mean over the period 1987–2017 of 491 mm and 447 mm, respectively). Thus, a Saharan dust deposition during snowfall is more likely

TABLE 4 | Mean relative ion composition of the mean overall annual depositions (MOAD) including all layers, as well as for SDLs and non-SDLs separately using the 10 μeq/l Ca^{2+} threshold.

	Cl^-	NO_3^-	SO_4^{2-}	Na^+	NH_4^+	K^+	Mg^{2+}	Ca^{2+}	H^+
All	8.5%	18.1%	13.9%	9.6%	16.5%	2.6%	2.7%	15.6%	12.9%
SDLs	7.2%	13.3%	11.0%	7.6%	12.7%	2.4%	4.1%	39.6%	2.1%
Non-SDLs	9.1%	18.7%	14.3%	10.3%	16.5%	2.8%	1.9%	11.9%	14.4%

TABLE 5 | Mean overall annual depositions (MOAD) in meq/m^2 and snow water equivalent (SWE) in mm of all years (1987–2017) and all layers, SDLs and non-SDLs as well as the absolute and relative contribution of the respective ions.

		MOAD (meq/m^2)	SWE (mm)	Cl^-	NO_3^-	SO_4^{2-}	Na^+	NH_4^+	K^+	Mg^{2+}	Ca^{2+}	H^+
	All	70.2	1579	6.0	12.7	9.8	6.7	11.6	1.8	1.6	10.9	9.0
Ca > 10 μeq/l	SDLs	10.0	172	0.7	1.3	1.1	0.8	1.3	0.2	0.4	3.9	0.2
		(14%)	(11%)	(11%)	(10%)	(11%)	(11%)	(12%)	(11%)	(25%)	(35%)	(2%)
	Non-SDLs	60.5	1420	5.5	11.3	8.6	6.2	10.0	1.7	1.2	7.2	8.7
		(86%)	(89%)	(89%)	(90%)	(89%)	(89%)	(88%)	(89%)	(75%)	(65%)	(98%)
Ca > 20 μeq/l	SDLs	8.7	125	0.5	1.0	0.9	0.5	0.9	0.1	0.3	4.4	0.1
		(11%)	(8%)	(7%)	(7%)	(8%)	(7%)	(8%)	(5%)	(16%)	(32%)	(1%)
	Non-SDLs	70.9	1508	6.3	13.0	10.9	6.8	11.0	1.8	1.6	9.3	10.3
		(89%)	(92%)	(93%)	(93%)	(92%)	(93%)	(92%)	(95%)	(84%)	(68%)	(99%)

in winter than in fall or spring. The increased number of SDLs in winter is also biased by single years (e.g., 1996 and 2014) where a huge number of layers were identified, all occurring in the winter period.

Influence of Saharan Dust Layers on the Relative Ion Composition

The mean relative ion composition was calculated for all layers together as well as for SDLs and non-SDLs separately. Results are presented in **Table 4**. Note that non-SDLs account for 89% of the snow water equivalent (**Table 5**) and hence also for the majority of the analyzed snow layers and the water deposited.

The relative ion composition of non-SDLs is almost identic to the ion composition if all layers are considered. The ratio between the relative contributions of most of the single ions within non-SDLs to those of the entire snow pack is slightly above 1 aside from Mg^{2+} and Ca^{2+} showing ratios of 0.7 and 0.8, respectively.

For SDLs, the relative ion composition is different to the ion composition of the entire snow pack. Mg^{2+} is slightly increased with a ratio between the relative contributions of SDLs to those of all layers of 1.4, whereas Ca^{2+} is much more increased with a ratio of 2.5. H^+ is markedly lower in SDLs with a ratio of only 0.1 between the relative contributions of non-SDLs to those of all layers. Contributions of all other ions are slightly decreased in SDLs, compared to the contributions if all layers are considered, with ratios between 0.7 and 0.9.

Influence of Saharan Dust Layers on Mean Annual Ion Deposition Loads

Table 5 lists the mean overall annual deposition (MOAD, sum of all ions analyzed) as well as the mean annual deposition loads of the respective ions and the snow water equivalent of the complete data set (1987–2017), calculated via averaging the respective annual values. The same was performed for the contribution of the SDLs and the non-SDLs, calculated as sum over all SDL or non-SDL layers of the respective years and averaging these annual values. In addition to the absolute values the relative contributions of SDLs and non-SDLs to the overall "MOAD," to the snow water equivalent and to the deposition loads of the single ions are listed as percentage values given in parenthesis. Note that the sums of SDL and non-SDL deposition loads need not match the overall annual loads. This is due to the fact that years without any SDL were not considered when splitting annual averages into SDL and non-SDL contributions. This approach was taken to base the averages of SDL and non-SDL contributions on the same data set, i.e., the same years. This accounts for the year to year variability, which has to be expected and which is discussed later.

For most of the single ions the contribution of SDLs and non-SDLs to the mean annual deposition load is similar to the respective contribution of the snow water equivalent, ranging between 10–12% and 88–90%, respectively. This indicates, that the concentrations of these ions is almost similar between SDLs and non-SDLs. Only Mg^{2+} and Ca^{2+} show much higher contributions of SDLs (25% and 35%, respectively), whereas H^+ shows a much lower contribution of only 2% compared to the snow water equivalent.

Interestingly, the contributions of the deposition loads of single ions but also of MOAD to the entire data set do not vary a lot when the Ca^{2+} threshold is increased from 10 to 20 μeq/l (**Table 5**). At first this seems surprising as the number of identified increments did go down by a factor of three when the threshold was increased. Still the deposition load is very much driven by the maximum concentrations which usually largely exceed 20 μeq/l. Thus annual deposition loads are not very much affected by the different thresholds.

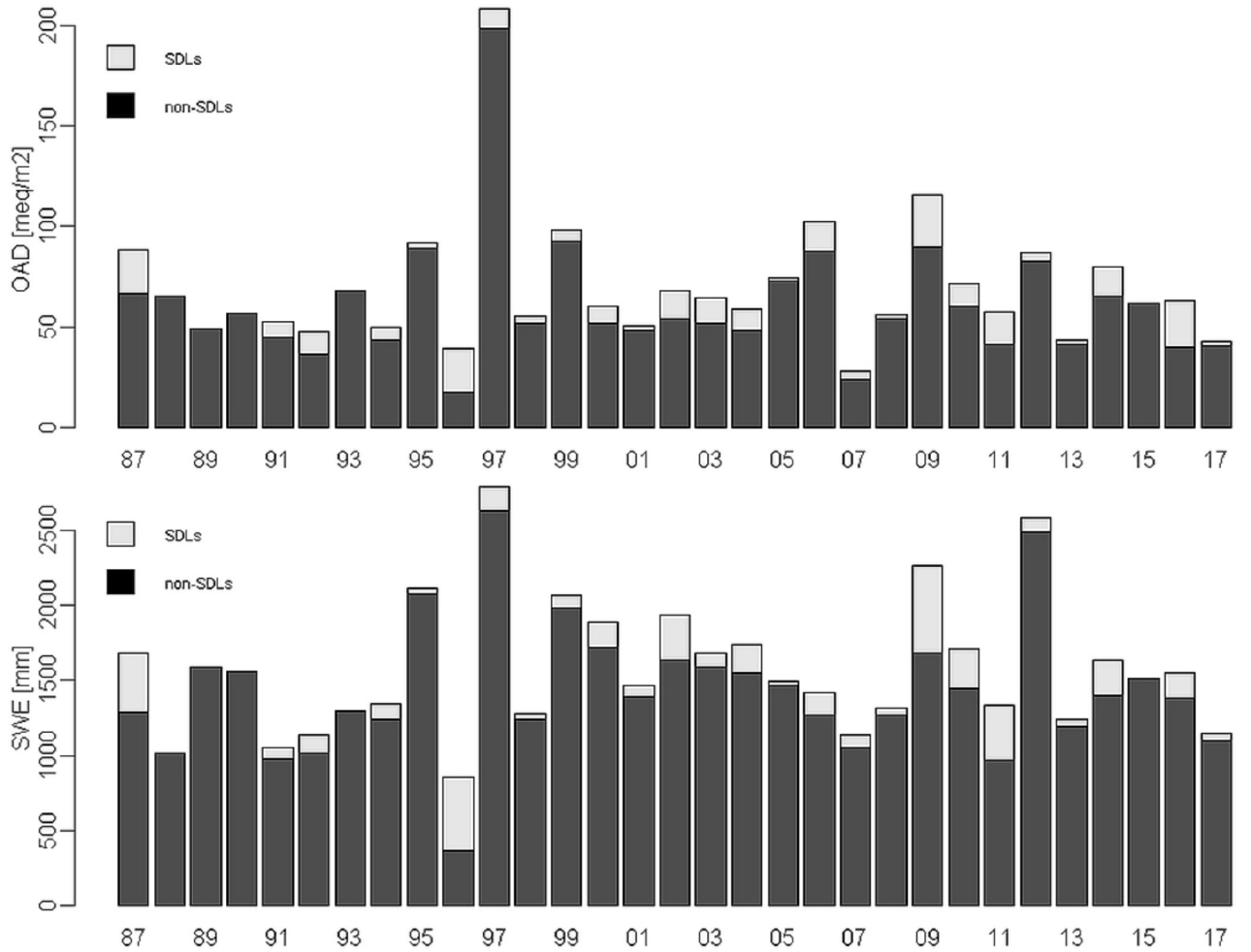

FIGURE 4 | Interannual variability of the overall annual deposition load including all ions (OAD) in meq/m^2 as well as of the snow water equivalent (SWE) in mm separated in the contribution of Saharan dust layers (SDLs) in gray and non-SDLs in black.

Interannual Variabilities of the Influence of Saharan Dust Layers on Ion Deposition

The interannual variability of the overall annual deposition load including all ions (OAD) as well as of the snow water equivalent is displayed in **Figure 4**.

The interannual variability of the OAD results for 9 of the 26 years with SD influence in a 13–19% contribution of SDLs whereas 2 years (1996 and 2016) show much higher contribution up to 55% and 36%, respectively (compare **Figure 4**). Likewise, also the annual depositions of the single ions show a high interannual variability with different trends. A detailed investigation of these annual trends, not quantifying the influence of deposited dust, can be found in Greilinger et al. (2016). Here results are exemplarily shown for Ca^{2+} and SO_4^{2-} in **Figure 5**. SO_4^{2-} depositions show a declining trend caused by decreasing emissions of sulfur dioxide (Greilinger et al., 2016). This trend is not altered if the deposition loads related to the deposition of SD would be deducted. Regarding the deposition of Ca^{2+} no significant time trend can be observed using the Mann-Kendall Test with a two-sided p-value below 5% for level of significance when the overall depositions are considered (Kendall's tau = 0.246 and 2-sided-p = 0.06). Also the contribution of SDLs to the annual Ca^{2+} deposition does not show any statistical trend (Kendall's tau = −0.119 and 2-sided-p = 0.38).

A boxplot shown in **Figure 6**, displaying the contribution of SDLs to the annual deposition of the single ions, reflects the interannual variability. The first box represents the interannual variability of the contribution of the SDLs to the annual snow water equivalent, showing a less than 10% for most of the years whereas outliers outside the upper whisker in the boxplot show 3 years where contributions were higher (1996, 2009, and 2011). In 1996 it was highest with 53%. Two years (1996 and 2006) were observed where all ions show a more than 25% contribution, for 1996 even more than 45%. For Ca^{2+} and Mg^{2+} more years were found with contributions of SDLs to the annual ion deposition load higher than 25%. For Ca^{2+} 16 years (1987, 1991, 1992,

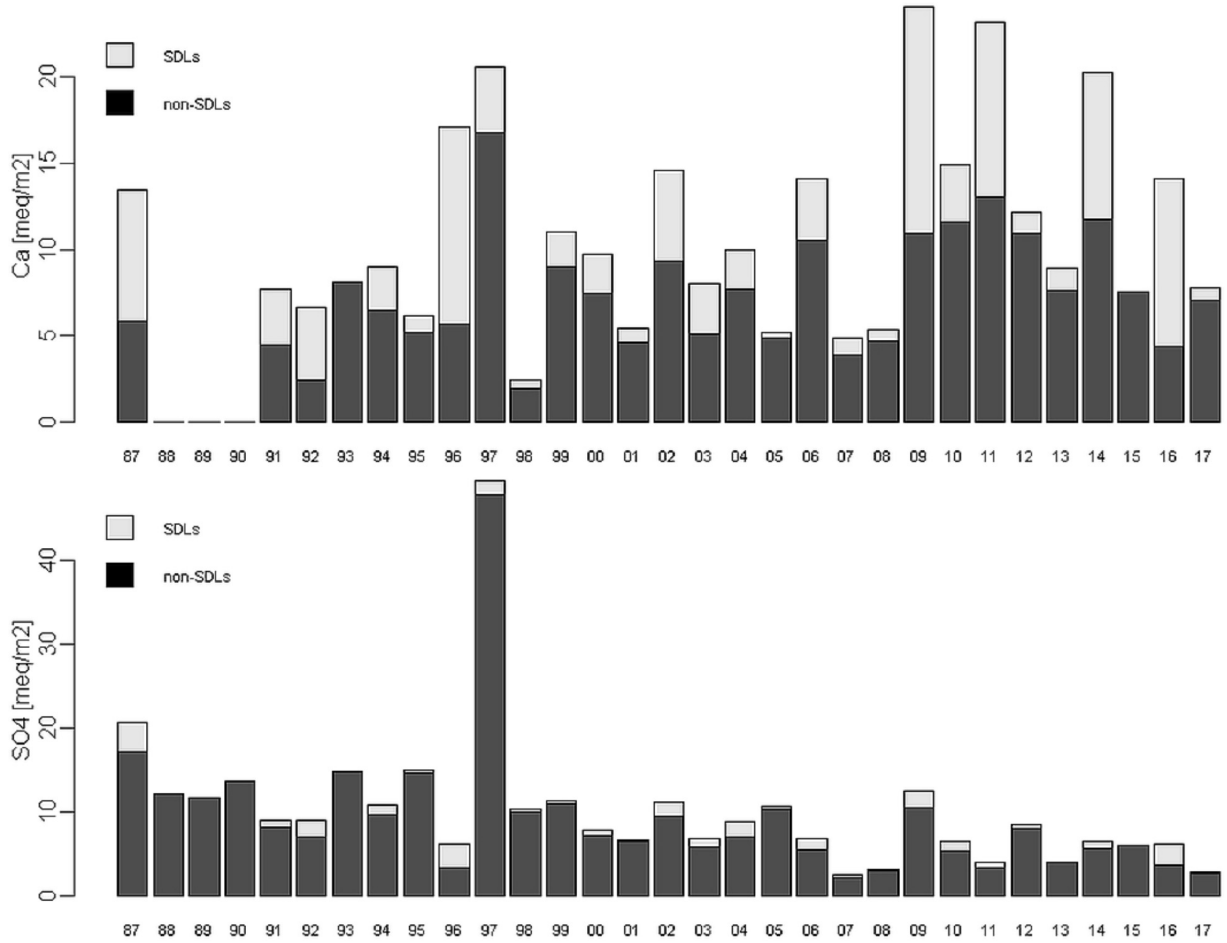

FIGURE 5 | Deposition of Ca^{2+} and SO_4^{2-} for all years of observation in meq/m^2 separated in the contribution of Saharan dust layers (SDLs) in gray and non-SDLs in black.

1994, 1996, 1998, 2000, 2002, 2003, 2004, 2006, 2007 2009, 2011, 2014, and 2016) where identified and five of these years (1987, 1992, 1996, 2009, and 2016) show contributions of more than 45%, in 1992, 1996, and 2016 even more than 60%. For Mg^{2+} 10 years (1987, 1991, 1996, 2001, 2002, 2003, 2007, 2011, 2014, and 2016) showed contributions above 25%, in 1987 and 2016 even more than 50%. Contributions for H^+ are always very low with maximum values of 5%. Contributions of single years (1996, 2004, 2009, and 2010) marked as outliers in **Figure 6** were higher with contributions of 33%, 18%, 14%, and 8%, respectively.

From these results we find 2 years, 1996 and 2016, which show remarkable high contributions of SDLs to the OAD as well as to the annual ion deposition. For both years red colored snow layers were already visually observed during sampling of the snow pack (**Table 2**) but the contribution of the SDLs to the annual snow water equivalent differ strongly with a contribution of 57% in 1996 but only 11% in 2016. This reveals, that in 1996 the contributions of SDLs to the annual ion deposition is high due to a high number of SDLs (12 layers) whereby the deposition load of these SDLs was not very high (Ca^{2+} concentrations between 15.0 and 42.7 μeq/l). In contrast to this, the high contributions of SDLs to the annual ion deposition in 2016 is associated to only three SDLs with very high Saharan dust input (Ca^{2+} concentrations of 24.4 μeq/l, 40.9 μeq/l, and 171.5 μeq/l).

The boxplot also underlines the main findings discussed before that the contribution of SDLs to the annual deposition loads is markedly different to the contribution of the snow water equivalent for Mg^{2+}, Ca^{2+}, and H^+ because these ions are most affected by Saharan dust. Regarding Cl^-, Na^+, and K^+, ions which are related to Saharan dust too but most likely have additional sources as well, the distributions are shifted to elevated contributions, but the differences to snow water equivalent are much less pronounced. The smallest influence can be seen for NO_3^-, SO_4^{2-}, and NH_4^+, but still 75th percentiles and whiskers reach up to markedly higher contributions of SDLs than can be expected due to the snow water equivalent of those layers.

DISCUSSION

In the following our results about the contribution of SDLs to the mean annual deposition loads are compared to those

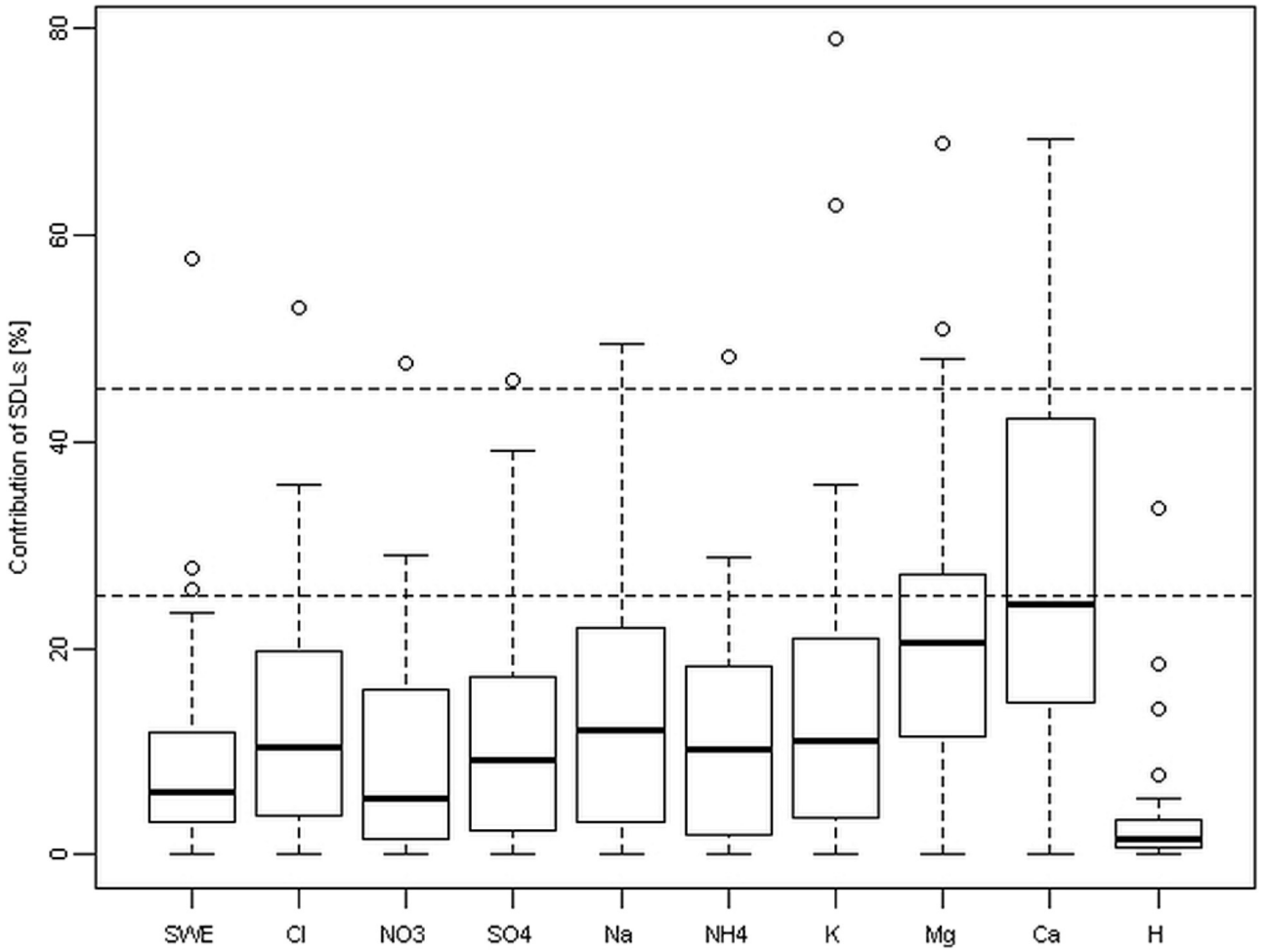

FIGURE 6 | Boxplot of the annual contributions of Saharan dust layers (SDLs) to the snow water equivalent (SWE) and the annual depositions of the single ions. The box represents the 25th and 75th percentile, the bold black line shows the median and whiskers extend to the most extreme data point which is no more than 1.5 times the interquartile range of the box. Dashed lines mark 25% and 45% contributions of SDLs.

of (Avila and Rodà, 1991), analyzing the dissolved nutrient amounts during red rains in Montseny Mountains, Spain from 1983 to 1988. They found that red rains are responsible for 46% Ca^{2+} input, between 20 and 25% for Na^+, K^+, Cl^-, and Mg^{2+} input and between 7 and 16% for SO_4^{2-}, NO_3^-, and NH_4^+ input featuring high interannual variability with coefficients of variations between 26 and 68% for the single ions. Still red rains contribute only 5% of the total annual precipitation for the study period, pointing to a higher relative influence of single events of red rains in Spain than in the present study. Rogora et al. (2004) report results on the impact of Saharan dust deposition on the long-term trends of atmospheric deposition in Italy from 1984 to 2002. They found that contribution of Saharan dust events to the annual precipitation amount was in average 10% whereas the mean contribution of the respective ions during these events where 43% Ca^{2+}, 20–24% of Mg^{2+}, Na^+, and Cl^- and 11–16% of NO_3^-, SO_4^{2-}, NH_4^+, and K^+, what is more similar to our results. Maupetit and Delmas (1994), investigating the snow chemistry of glaciers in the French Alps from 1989 to 1991, found alkaline samples to contribute 19% on average over all years, representing between 22 and 52% of the ionic load, with the highest amount for Ca^{2+}. Values of Maupetit and Delmas (1994) are highest, most likely due to the fact that they did not distinguish between alkaline samples originating from Saharan dust or from increased NH_4^+ concentrations, both acting as buffering agents. If no Ca^{2+} criterion would have been used in the present study the number of affected increments would have been more than threefold.

Regarding the nutrient input via Saharan dust the importance of Ca^{2+}, Mg^{2+}, and K^+ is mentioned in literature (e.g., Avila et al., 1998). Our data set shows that the input of Ca^{2+} and Mg^{2+} definitely is driven by long-range transport of mineral dust, while no marked effect becomes visible for K^+. In this case other sources, e.g., the more regional influence of combustion processes, are more important. The same is the case for Na^+, another ion, whose input could have been driven by mineral dust (e.g., Swap et al., 1992; Rizzolo et al., 2017).

Additionally to the influence of Saharan dust on ion deposition loads we suggest that Saharan dust in snow may

not only directly influence microbiology by acting as fertilizer and additional nutrient input to increase biomass but rather influences the metabolism, respiration, and productivity of microbes (Pulido-Villena et al., 2008; Reche et al., 2009; Schulz et al., 2012). In this respect, the changed acidity could be an important parameter as well. We found the pH to be distinctly different in SDLs compared to unaffected snow layers, providing distinctly different habitat conditions for microorganisms surviving within high alpine snow packs. Also the community diversity in high alpine snow is changed due to Saharan dust input (Zhang et al., 2008; Chuvochina et al., 2011). Due to the fact that Saharan dust introduces a variety of bacteria and microbial species to areas far away from their origin, it can be assumed that, especially in remote alpine snow, the accomplished input of Saharan dust simulate the natural habitat of those microbes so they can survive in very harsh and contrary conditions to their original habitat.

SUMMARY AND CONCLUSION

We investigated the intensity and frequency of Saharan dust deposited in high alpine snow retrospectively for a unique long-term data set of high alpine snow chemistry.

Based on a chemical criterion (pH $>$ 5.6 and Ca^{2+} concentration $>$ 10 μeq/l) we provide a robust method to identify SDLs within high alpine snow packs. Results for the use of a higher Ca^{2+} threshold (20 μeq/l) show, that it hardly affect the annual deposition loads whereas the number of identified layers goes down.

While contributions of SDLs and unaffected layers (10–12% and 88–89%, respectively) to the deposition load of Cl^-, NO_3^-, SO_4^{2-}, Na^+, NH_4^+, and K^+ is similar to the contribution of the snow water equivalent (11% and 86%, respectively), markedly elevated contributions of SDLs were observed for Mg^{2+} (25%) and Ca^{2+} (35%), while the impact of H^+ becomes negligible (2%). Also the relative ion composition in SDLs underlines the influence on Mg^{2+}, Ca^{2+}, and H^+.

Generally SO_4^{2-} depositions show a declining trend caused by decreasing emissions of sulfur dioxide but this trend is not altered if the deposition loads related to the deposition of Saharan dust would be deducted. Regarding the deposition of Ca^{2+} no significant time trend was observed at all.

Using the suggested Ca^{2+} threshold of 10 μeq/l, only 2 out of 28 investigated years without Saharan dust influence were observed. Two thirds of the affected years showed even more than one SDL. This is the case, although a 3-year comparison of the identified SDLs using backward trajectories and on-line aerosol measurements showed that we might miss weak events.

An estimation of the contribution of Saharan dust events to the chemical variability of the ecosystems is not easy due to lack of quantitative studies in remote areas but cannot be neglected. Our results provide relevant input not only on ion deposition loads. They can be used for further investigations and conclusions on the influence of Saharan dust on the albedo of snow and glacier surfaces, on the biogeochemistry of high alpine snow as well as on the microbiology of remote areas.

AUTHOR CONTRIBUTIONS

MG and AK-G conceived the study. MG processed the data and wrote the manuscript together with AK-G. GS performed and evaluated the aerosol sampling at the site and calculated the DI. KB-S and PS performed the backward trajectory analysis. WS was part of the team initiating the snow chemistry monitoring and ensuring ongoing sampling for most of the years. All co-authors commented on the results and on the manuscript content.

ACKNOWLEDGMENTS

The long-term monitoring was developed during the EUROTRAC-ALPTRAC Project and ongoing monitoring is financially supported by the BMLFUW. Thanks go to the members of the various sampling teams responsible for field work and colleagues conducting the chemical analysis during the nearly 31-year period. Furthermore, we would like to acknowledge the help from Claudia Flandorfer and Marcus Hirtl for WRFChem model simulations, Anton Neureiter for drawing the site map in GIS, Roland Koch for TAWES data and Daniela Kau for part of the analytical work regarding the GOK2016 data set. Aerosol measurements are carried out in cooperation with Umweltbundesamt. Finally we acknowledge the TU Wien University Library for financial support through its Open Access Funding Program.

SUPPLEMENTARY MATERIAL

The Supplementary Material for this article can be found online at: https://www.frontiersin.org/articles/10.3389/feart.2018.00126/full#supplementary-material

REFERENCES

Avila, A., Alarcón, M., and Queralt, I. (1998). The chemical composition of dust transported in red rains-its contribution to the biogeochemicl cycle of a holm oak forest in Catalonia (Spain). *Atmos. Environ.* 32, 179–191. doi: 10.1016/S1352-2310(97)00286-0

Avila, A., and Rodà, F. (1991). Red rains as major contributors of nutrients and alkalinity to terrestrial ecosystems at Montseny (NE Spain). *Orsis* 6, 215–229.

Chuvochina, M. S., Marie, D., Chevaillier, S., Petit, J.-R., Normand, P., Alekhina, I. A., et al. (2011). community variability of bacteria in alpine snow (mont blanc) containing saharan dust deposition and their snow colonisation potential. *Microbes Environ.* 26, 237–247. doi: 10.1264/jsme2.ME11116

Coen, M. C., Weingartner, E., Schaub, D., Hueglin, C., Corrigan, C., Schwikowski, M., et al. (2003). Saharan dust events at the Jungfraujoch: detection by wavelength dependence of the single scattering albedo and analysis of the events during the years 2001 and 2002. *Atmos. Chem. Phys. Discuss.* 3, 5547–5594. doi: 10.5194/acpd-3-5547-2003

Das, R., Das, S. N., and Misra, V. N. (2005). Chemical composition of rainwater and dustfall at Bhubaneswar in the east coast of India. *Atmos. Environ.* 39, 5908–5916. doi: 10.1016/j.atmosenv.2005.06.030

De Angelis, M., and Gaudichet, A. (1991). Saharan dust deposition over mont blanc (French Alps) during the last 30 years. *Tellus B* 43, 61–75. doi: 10.3402/tellusb.v43i1.15246

Field, J. P., Belnap, J., Breshears, D. D., Neff, J. C., Okin, G. S., Whicker, J. J., et al. (2010). The ecology of dust. *Front. Ecol. Environ.* 8, 423–430. doi: 10.1890/090050

Gabbi, J., Huss, M., Bauder, A., Cao, F., and Schwikowski, M. (2015). The impact of Saharan dust and black carbon on albedo and long-term mass balance of an Alpine glacier. *Cryosphere* 9, 1385–1400. doi: 10.5194/tc-9-1385-2015

Goudie, A. S., and Middleton, N. J. (2001). Saharan dust storms: nature and consequences. *Earth Sci. Rev.* 56, 179–204. doi: 10.1016/S0012-8252(01)00067-8

Greilinger, M., Schöner, W., Winiwarter, W., and Kasper-Giebl, A. (2016). Temporal changes of inorganic ion deposition in the seasonal snow cover for the Austrian Alps (1983–2014). *Atmos. Environ.* 132, 141–152. doi: 10.1016/j.atmosenv.2016.02.040

Grell, G. A., Peckham, S. E., Schmitz, R., McKeen, S. A., Frost, G., Skamarock, W. C., et al. (2005). Fully coupled "online" chemistry within the WRF model. *Atmos. Environ.* 39, 6957–6975. doi: 10.1016/j.atmosenv.2005.04.027

Gruber, N., and Sarmiento, J. L. (1997). Global patterns of marine nitrogen fixation and denitrification. *Glob. Biogeochem. Cycles* 11, 235–266. doi: 10.1029/97GB00077

Kuhn, M. (2001). The nutrient cycle through snow and ice, a review. *Aquat. Sci. Res. Boundaries* 63, 150–167. doi: 10.1007/PL00001348

Marchetto, A., Mosello, R., Psenner, R., Bendetta, G., Boggero, A., Tait, T., et al. (1995). Factors affecting water chemistry of alpine lakes. *Aquat. Sci.* 57, 81–89. doi: 10.1007/BF00878028

Maupetit, F., and Delmas, R. J. (1994). Snow chemistry of high altitude glaciers in the French Alps. *Tellus B Chem. Phys. Meteorol.* 46, 304–324. doi: 10.3402/tellusb.v46i4.15806

Moulin, C., Lambert, C. E., Dulac, F., and Dayan, U. (1997). Control of atmospheric export of dust from North Africa by the North Atlantic Oscillation. *Nature* 387, 691–694. doi: 10.1038/42679

Prospero, J. M. (1996). "Saharan dust transport over the North Atlantic Ocean and Mediterranean: an overview," in *Impact Desert Dust Mediterr*, eds S. Guerzoni and R. Chester (Alphen aan den Rijn: Kluwer Academic Publishers), 133–151. doi: 10.1007/978-94-017-3354-0_13

Psenner, R. (1999). Living in a dusty world: airborne dust as a key factor for alpine lakes. *Water Air Soil Pollut.* 112, 217–227. doi: 10.1023/A:1005082832499

Pulido-Villena, E., Wagener, T., and Guieu, C. (2008). Bacterial response to dust pulses in the western Mediterranean: implications for carbon cycling in the oligotrophic ocean: bacterial response to dust pulses. *Glob. Biogeochem. Cycles* 22:GB1020. doi: 10.1029/2007GB003091

Reche, I., Ortega-Retuerta, E., Romera, O., Villena, E. P., Baquero, R. M., and Casamayor, E. O. (2009). Effect of Saharan dust inputs on bacterial activity and community composition in Mediterranean lakes and reservoirs. *Limnol. Oceanogr.* 54, 869–879. doi: 10.4319/lo.2009.54.3.0869

Rizzolo, J. A., Barbosa, C. G. G., Borillo, G. C., Godoi, A. F. L., Souza, R. A. F., Andreoli, R. V., et al. (2017). Soluble iron nutrients in Saharan dust over the central Amazon rainforest. *Atmos. Chem. Phys.* 17, 2673–2687. doi: 10.5194/acp-17-2673-2017

Rogora, M., Mosello, R., and Marchetto, A. (2004). Long-term trends in the chemistry of atmospheric deposition in Northwestern Italy: the role of increasing Saharan dust deposition. *Tellus B Chem. Phys. Meteorol.* 56, 426–434. doi: 10.3402/tellusb.v56i5.16456

Schauer, G., Kasper-Giebl, A., and Močnik, G. (2016). Increased PM concentrations during a combined wildfire and Saharan dust event observed at high-altitude sonnblick observatory, Austria. *Aerosol Air Qual. Res.* 16, 542–554. doi: 10.4209/aaqr.2015.05.0337

Schulz, M., Prospero, J. M., Baker, A. R., Dentener, F., Ickes, L., Liss, P. S., et al. (2012). Atmospheric transport and deposition of mineral dust to the ocean: implications for research needs. *Environ. Sci. Technol.* 46, 10390–10404. doi: 10.1021/es300073u

Schwikowski, M., Döscher, A., Gäggeler, H. W., and Schotterer, U. (1999). Anthropogenic versus natural sources of atmospheric sulphate from an alpine ice core. *Tellus B Chem. Phys. Meteorol.* 51, 938–951. doi: 10.3402/tellusb.v51i5.16506

Stohl, A., Haimberger, L., Scheele, M. P., and Wernli, H. (2001). An intercomparison of results from three trajectory models. *Meteorol. Appl.* 8, 127–135. doi: 10.1017/S1350482701002018

Swap, R., Garstang, M., Greco, S., Talbot, R., and Kållberg, P. (1992). Saharan dust in the Amazon Basin. *Tellus B* 44, 133–149. doi: 10.1034/j.1600-0889.1992.t01-1-00005.x

Weil, T., De Filippo, C., Albanese, D., Donati, C., Pindo, M., Pavarini, L., et al. (2017). Legal immigrants: invasion of alien microbial communities during winter occurring desert dust storms. *Microbiome* 5:32. doi: 10.1186/s40168-017-0249-7

Winiwarter, W., Puxbaum, H., Schöner, W., Böhm, R., Werner, R., Vitovec, W., et al. (1998). Concentration of ionic compounds in the wintertime deposition: results and trends from the Austrian Alps over 11 years (1983–1993). *Atmos. Environ.* 32, 4031–4040. doi: 10.1016/S1352-2310(97)00252-5

Zhang, S., Hou, S., Wu, Y., and Qin, D. (2008). Bacteria in Himalayan glacial ice and its relationship to dust. *Biogeosci.* 5, 1741–1750. doi: 10.5194/bg-5-1741-2008

Conflict of Interest Statement: The authors declare that the research was conducted in the absence of any commercial or financial relationships that could be construed as a potential conflict of interest.